Identification and calibration of the interaction matrix parameters for AO and MCAO systems

Benoit Neichel[a], Amelie Parisot[b], Cyril Petit[b], Thierry Fusco[b],François Rigaut[a]

[a] Gemini Observatory, c/o AURA, Casilla 603 La Serena, Chile
[b] ONERA, DOTA, Unité HRA, 29 avenue de la division Leclerc, 92322 Chatillon, France

ABSTRACT

New tomographic Adaptive Optics (AO) concepts require a good knowledge of the system geometry and characteristics. These parameters are used to feed the tomographic reconstructors. In this paper we present a method to precisely identify the parameters required to construct an accurate synthetic set of models such as influence functions, mis-registrations, directions of analysis or altitude of the DMs. The method is based on a multi-parameter fit of the interaction matrix. This identification method finds also its application in high contrast AO systems, such as SPHERE : in that case it is used as a diagnostic tool in order to precisely realign the system. The method has been tested and successfully implemented on HOMER, SPHERE and GeMS. Experimental results for these three systems are presented.

Keywords: Calibration, interaction matrix

1. INTRODUCTION

Until recently, almost all the Adaptive Optics (AO) systems were classical AO systems, using a single Deformable Mirror (DM) and a single wave-front sensor (WFS), and working on-axis. In such configuration, the relation between the phase introduced by the DM and the WFSs can be measured directly, through an interaction matrix (noted iMat in the following). Measured iMat are convenient as they include all the actual system characteristics and idiosyncrasies, such as WFS response and gain, DM actuator gains, optical misalignment, etc... So even if an AO system is not perfectly aligned, or well characterized, these effects are taken into account when one measures the iMat. Looking at the problem from the other side, this measured iMat could be used as a tool to evidence optical mis-alignments and monitor system stability. This, however, requires tools to interpret the iMat and retrieve such information.

New generation of AO systems including extremely high-order systems or wide field systems are bringing new constraints. In the case of high order system like SPHERE[1] or GPI[2] maintaining a good registration between the DM actuators and the WFS sub-apertures is critical, as performance loss and loop instabilities will start to appear for mis-registration as small as 10% of an actuator pitch. Measuring an iMat may not be convenient for systems with a large number of actuators as it is time consuming. New methods based on the Hadamard approach have been developed to speed up the iMat measurement.[3,4] Analyzing these iMat in order to monitor mis-registration and calibration drifts is then very important. In the case of wide field system (e.g. GeMS[5] or ATLAS[6]) the situation is more complex, as the tomographic reconstructor requires an iMat for many directions. On top of mis-registration, the direction of analysis and correction of the turbulence should be known for an accurate tomographic reconstruction.

What are the parameters that should be determined ?
A tomographic reconstructor (let's call it W) can usually be divided in two contributors:[7]

$$\mathbf{W} = \mathbf{P_{opt}} \mathbf{W_{tomo}} \tag{1}$$

These two matrices being defined by:

Further author information: (Send correspondence to bneichel@gemini.edu or amelie.parisot@onera.fr)

Adaptive Optics Systems III, edited by Brent L. Ellerbroek, Enrico Marchetti, Jean-Pierre Véran, Proc. of SPIE Vol. 8447, 84475N · © 2012 SPIE · CCC code: 0277-786/12/$18 · doi: 10.1117/12.925277

- A tomographic reconstructor $\mathbf{W_{tomo}}$ corresponding to a step of phase reconstruction into a volume. This operator only depends on the GS and WFS geometry.
- A projector $\mathbf{P_{opt}}$ of the estimated volume reconstruction on the DMs. This operator only depends on the altitude conjugation of the DMs and the direction of optimizations.

Let's use the following notations:

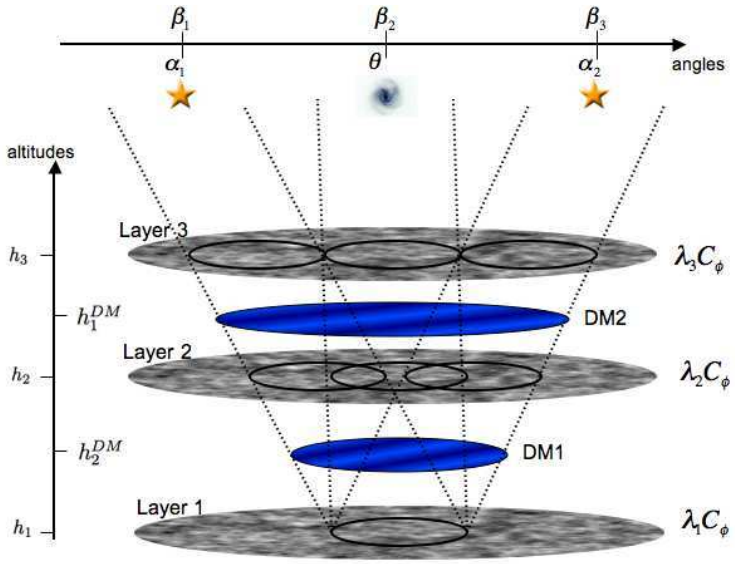

Figure 1. Illustration of system geometry and notations used.

The measurement is performed with several WFSs, each WFS looking at one Guide Star. The GS positions are given by $\alpha = \alpha_i$. The correction is performed by N_{DM} DMs, optically conjugated to altitudes h_n^{DM}. The FoV of interest, where the correction has to be optimized, is discretized into N_{ang} angles $\beta = \beta_j$. Neglecting the time aspect, the measurement done by the WFSs $\phi^{\mathbf{mes}}$, can be described by the following equation:

$$\phi^{\mathbf{mes}} = \mathbf{M}(\mathbf{P}_\alpha^{\mathbf{L}}\varphi_{\mathbf{turb}} - \mathbf{P}_\alpha^{\mathbf{N}}\mathbf{N}\mathbf{u}) + \mathbf{b} \tag{2}$$

where $\mathbf{M}$ is a model of the WF sensing operation, $\mathbf{P}_\alpha^{\mathbf{L}}$ projects the L turbulent phases seen in the α directions in the pupil, $\mathbf{P}_\alpha^{\mathbf{N}}$ projects the n correction phases produced by the DMs in the same α directions, $\mathbf{N}$ is a model of the DMs influence functions, u are the voltages sent to the DMs, and b is the WFS noise.

Assuming an MMSE like reconstruction, we can detail the two matrices defined in equation 1:

$$\begin{aligned}
\mathbf{W_{tomo}} &= \left[(\mathbf{M}\mathbf{P}_\alpha^{\mathbf{L}})^{\mathbf{T}}(\mathbf{C_b^{noise}})^{-1}\mathbf{M}\mathbf{P}_\alpha^{\mathbf{L}} + \mathbf{C}_{\varphi_\mathbf{n}}^{-1}\right]^{-1}(\mathbf{M}\mathbf{P}_\alpha^{\mathbf{L}})^{\mathbf{T}}(\mathbf{C_b^{noise}})^{-1} \\
\mathbf{P_{opt}} &= \left[\langle(\mathbf{P}_{\beta_\mathbf{j}}^{\mathbf{DM}}\mathbf{N})^{\mathbf{T}}\mathbf{P}_{\beta_\mathbf{j}}^{\mathbf{DM}}\mathbf{N}\rangle_\beta\right]^{-1}\langle(\mathbf{P}_{\beta_\mathbf{j}}^{\mathbf{DM}}\mathbf{N})^{\mathbf{T}}\mathbf{P}_{\beta_\mathbf{j}}^{\mathbf{L}}\rangle_\beta
\end{aligned} \tag{3}$$

Hence, the parameter that one must know to be able to construct a tomographic reconstructor are the following:

- $\mathbf{N}$: the DMs influence functions
- $\mathbf{M}$: the WF sensing model (including e.g. mis-registrations)
- $\mathbf{P}_\alpha$: the projection in the direction of analysis

- $\mathbf{P}_\beta$: the projection in the direction of optimization
- h_n^{DM} the altitude of the DMs

The relative geometry between the various components is also of significant interest.

What is the sensibility of the tomography to these parameters ?

The exact sensitivity of the system performance to misalignment and calibration errors affecting all these parameters will of course depend on the system itself, the control law, and requires an extensive study. Still, some well known rule of thumbs have been validated in various systems analysis and lead to the following first tolerances:

- relative translation between DM and WFS is acceptable up to 1/10 of a sub-aperture,
- relative rotation between DM and WFS is acceptable up to 1/10 of an edge sub-aperture,
- relative position of pupil footprint in the DM meta-pupil (for MCAO systems for instance) follows the same sensitivity.

How can we determine all the matrices required for the tomography ?

Following the same formalism as above, and assuming a multi-DMs, multi-WFS systems, an interaction matrix would be described by:

$$\mathbf{iMat} = \mathbf{M}\mathbf{P}_\theta^{\mathbf{N}}\mathbf{N} \tag{4}$$

where θ are the directions in which one can measure the iMat. For practical reasons, iMat is only measured in specific directions which may be different from the ones required to build the tomographic reconstructor. In general, iMat is measured with calibration sources installed on the AO bench, and usually $\theta == \alpha$. However, this might not be always the case, especially in systems using NGS, the constellation will be different for every targets, and measuring the iMat for all the configuration is not possible. In that case, a first solution proposed by Kolb et al.[8] was to interpolate the iMat, based on a reference iMat measured in specific directions. Another possibility is to measure the interaction matrix on-sky for each target, even though it consumes valuable telescope time. Another approach is building a numerical model of the AO components, and working with synthetic matrices.[9] The main advantage of these synthetic matrices are that they are noiseless, and for systems with a large number of degrees of freedom, the stability and accuracy of the inversion process critically depends on the signal-to-noise of the input matrices. Synthetic matrices can be readily pre-computed, which is very relevant if the geometry is dependent on operational parameters. Synthetic matrices however can not be generated without any precautions, and a necessary set of conditions are that:

- DM actuator gains and, if necessary, WFS sub-aperture gains (centroid gains, if using quad-cells) have to be calibrated).
- The DMs influence functions have to be adjusted to match the actual ones.
- Mis-registration and system geometries (GS directions, DM altitudes) has to be factored in.

Moreover, having a way to calibrate these models with the real hardware, and with the real bench environment then becomes primordial. In this paper, we present a method for the parameter identification process, based on a minimization algorithm using the interaction matrix as input data. This method gives a way to calibrate the numerical models, and build the set of necessary matrices. Two remarks are important to emphasize at that point:

- the models that can be identified from the analysis of the iMat do not include anything related to the turbulence itself. Some matrices required to build the tomographic reconstructors include some knowledge of the turbulence altitude and strength. From numerical models, it has been shown in previous studies[10,11] that the tomographic reconstruction is very sensitive to model errors in altitude and number of layers used in the volume estimation. The information on the turbulence profile can be acquired by other methods ([12–14]) ;
- in this paper, we are not addressing any dynamical changes of the registration. In a real system, the mis-registration may change with flexures, local pupil distortion or even motor (encoder) malfunctions.[15] Many AO systems include some kind of field selection, or zoom mechanism to compensate for the LGS range variations and differential flexures between the DM(s) and WFS(s). These mechanisms can not behave perfectly, and induce mis-registrations. Addressing dynamical registration errors is out of the scope of this paper. It can be done by more sophisticated methods, like Bechet et al.[16]

The paper is organized as follow: in section 2 we introduce the method and we validate it with some simulations, in section 3 we introduce the three systems on which we tried it and section 4 shows the experimental results.

2. IDENTIFICATION METHOD

2.1 Description of the method

Let *params* be the parameters to be identified from an experimental interaction matrix $\mathbf{iMat}_{exp}(params, noise)$. Since any system mis-calibration has an effect on this matrix, parameters will be identified thanks to an iterative comparison between the experimental matrix and the estimated one. The latter is recalculated at each iteration with parameters which are adjusted to minimize the Froebenius norm between the two matrices. This criterion can be written:

$$\begin{aligned} criterion &= ||\mathbf{W}\left(\mathbf{iMat}_{exp}(params, \sigma_{bruit}) - \mathbf{iMat}_{est}(par\hat{a}ms)\right)||^2 \\ criterion &= \textstyle\sum_{i,j}\left(w[i,j](\mathbf{iMat}_{exp}[i,j] - \mathbf{iMat}_{est}[i,j])\right)^2 \end{aligned} \tag{5}$$

where $\mathbf{W}$ is a weight function and $m[i,j]$ represents the term set at the ith row and the jth column of $\mathbf{M}$. A multi-variable minimization algorithm is used to perform the estimation. We use a Levenberg-Marquardt type algorithm.[17] Based on this minimization, we have developed two approaches depending on the kind of calibration needed.

In the first approach, the free parameters are the positions and Influence Functions (IF) of each actuator. For each actuator, we extract the corresponding line of the experimental iMat, and we adjust its mis-registration and shape to find the right measurement. For instance, for GeMS we consider IF with the following analytical form :

$$IF = sinc(x/a) * sinc(y/a) * exp(-(x/b)^2. - (y/b)^2.)) \tag{6}$$

where a and b are left free during the optimization procedure. This is done for each actuator of the different DMs, and for each WFS. To speed-up the process, only the first subapertures around the actuators of interest are used in the fit thanks to a binary weight map. The result of this fit is a map of mis-registration and IF for each couple WFS/DM. The registration maps are projected on an orthogonal basis formed by a two direction translation (Tip / Tilt), a magnification (Focus) and a Rotation for each WFS on each DM. For a multi-WFS configuration, anything which is common to all WFS in terms of translation can be compensated by shifting the DM, so can be interpreted as a DM mis-alignment. Once we subtract this common part, we are left with differential mis-registration between the WFS. To understand the origin of this differential mis-registration, we project it on 2 terms: a rotation and a magnification. The global rotation is due to a rotation of the DM, and can be subtracted. Everything left would likely be due to errors in the analysis directions, however, the projection of this differential mis-registration on a magnification term could also be interpreted as an error on the DM altitude. Let's illustrate this on a simple example. If we take the case of a DM in altitude, and 2

directions of analysis, a shift in altitude of the DM will create a mis-registration in +X for the WFS on the left, and -X for the one on the right. Shifting both direction of analysis by the same amount would produce an exact same iMat, and we have no ways to disentangle them. Let's consider a realistic case with sub-apertures of 0.5m, a DM in altitude conjugated at 10km, and a constellation angle of 1arcmin. If the DM is 200m off, that would produce a mis-registration of 0.06subaperture, which could also be interpreted as an angle of 0.6arcsec. This is an intrinsic limitation of the method. Obviously, the more DMs used to measure the iMat, the more constraints are added to disentangle both effects. It is also important to note that this degeneracy is solved for systems working with sources which are not at infinity (e.g. LGS), or for AO systems working with non-collimated beams (e.g. HOMER) as a DM altitude error will produce an additional magnification error term, common for all the WFSs.

Once all the effects due to the DM and direction of analysis have been subtracted on the mis-registration maps, we are left with the lenslet defaults which is a good indicator of their optical quality. This gives us an information on the intrinsic lenslet local alignment issues, which can not be adjusted by any alignments. But this residual map can be introduced in the synthetic models when they are generated, and it also provides a way to monitor the aging of this optical element.

In the second approach, we fix the IF and location of each actuator, and the free parameters are now the DM position (Tip/Tilt and altitude) and the WFS pointing directions. The WFS directions are defined by their polar coordinates (ρ,Ψ), where ρ is the polar radius, and Ψ the polar angle as defined in figure 2.

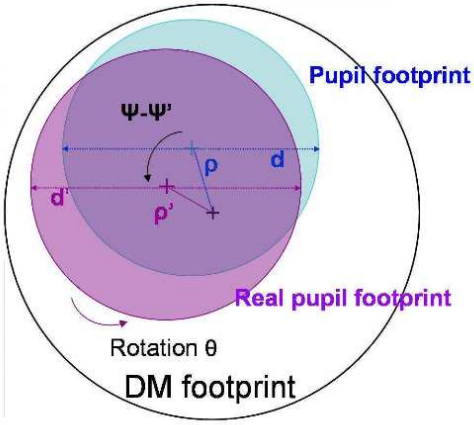

Figure 2. Altitude DM footprint. Analysis direction is labeled with its polar coordinates (ρ,Ψ).

When the IF are not required, this second approach provides much faster results.

2.2 Validation on simulation

We have tested the method with different simulations cases. Simulations results have been presented in a previous paper.[18] We recall here the main results. The identification process converges well. The criterion is plotted on figure 3.1, with respect to the translation value, for a non-weighted criterion and for a weighted criterion. Two noise conditions are presented : a very poor one SNR=4, and a good one SNR=100. Note that SNR is defined by :

$$\mathrm{SNR} = \frac{\max(\mathbf{iMat})}{\sigma_{\mathrm{noise}}}, \tag{7}$$

where σ_{noise} is the noise standard deviation. In all cases the criterion is convex and the global minimum corresponds to the introduced translation. The convexity of the criterion has also been checked with respect to rotation and to magnification. On figure 3.2 the mean of the absolute value of the estimation error (100

iMat population for each SNR) is plotted. And even at low SNR conditions this estimation error is very low. For a simulated matrix with a translation in one direction of 10% of the sub-pupil, a rotation of $\pi/16$, and a magnification of 1.01, the absolute value of the error of estimation for a SNR of 15 (uncertainty is defined at $3.\sigma$) is 8.10^{-3} ± 0.03 sub-aperture for translation, $2.5.10^{-3}$ ± 0.03 edge sub-aperture for rotation, and 5.10^{-4} ± 0.002 for the magnification.

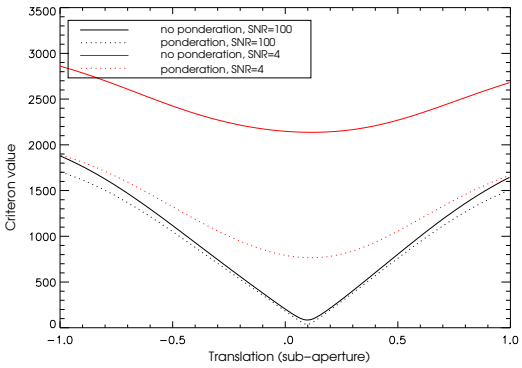

3.1 Criterion function of the translation value with a fixed value of rotation. The introduced translation is 0.1 sub-aperture.

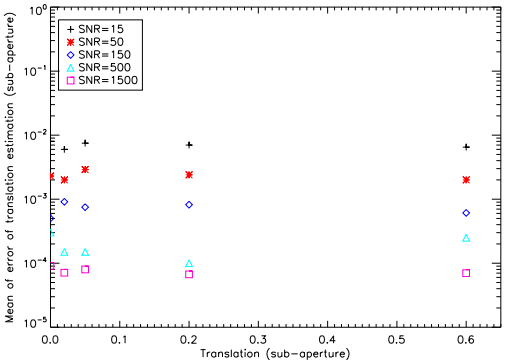

3.2 Algorithm performance: mean of the absolute value of the error of estimation of translation is plotted vs translation values, for different values of SNR. Uncertainty defined at $3*\sigma$ (σ is the standard deviation) is 0.03, 0.009, 0.003, 0.009 and 0.003 sub-aperture repectively for SNR of 15, 50, 150, 500 and 1500

Figure 3. Pseudo-experimental interaction matrix has been simulated with a translation in one direction of 10% of the sub-pupil, a rotation of $\pi/16$, and a magnification of 1,01.

In a Wide Field AO (WFAO) system, like Multi-conjugate AO (MCAO), one or several DMs are conjugated in altitude. We recall that the parameters to identify then correspond to the area analyzed by the WFS, defined by the polar coordinates ρ, Ψ and h, the DM altitude. The three parameters ρ, Ψ, h are simultaneously adjusted by the minimization algorithm. Figure 4 shows the performance of the algorithm to retrieve these three parameters on a simulation case, for $\Psi = 45$ degrees, ρ=11.7" and h=5000 m. The estimation of the altitude is quite the same for all considered values of Ψ and ρ: the altitude is an independent parameter. On the contrary, ρ and Ψ are coupled. The larger ρ is, the larger the standard deviation of the error on ρ is and the lower the standard deviation of the error on Ψ is. The impact of a rotation Ψ is indeed higher when the distance to the centre is larger.

The very good precision on parameters estimation obtained even in bad SNR conditions validates the identification process and is very encouraging for the implementation of this process on a bench.

3. HOMER, GEMS AND SAXO

In this paper we have tested and used the method on 3 different AO benches, respectively HOMER, GeMS and SAXO. We give some background informations about these systems in the following:

3.1 The Homer test bench

HOMER bench is a laboratory bench devoted to implementation and validation of WFAO concepts such as Ground Layer AO (GLAO), Laser Tomography AO (LTAO) or MCAO. After two years of design and integration, HOMER is now fully operational and has begun to be exploited in 2009. See[19] for a detailed description of the bench. Just a brief reminder is done about its set-up.

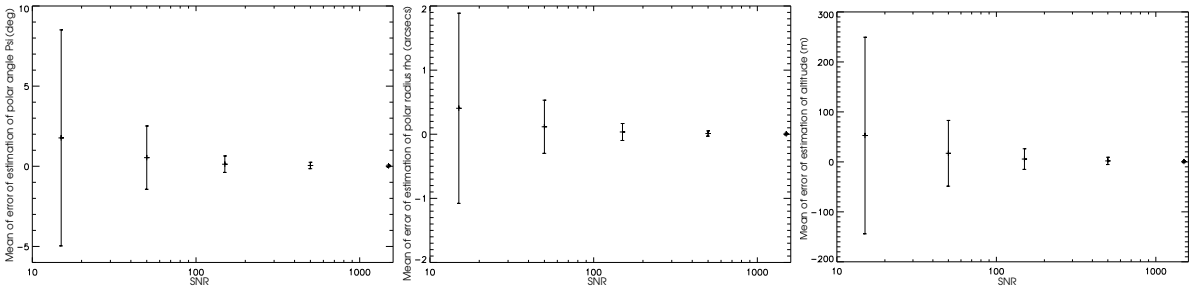

4.1 Mean of the absolute value of the error on estimation of Ψ function of the value of Ψ in degrees.

4.2 Mean of the absolute value of the error on estimation of ρ function of the value of ρ in arcsecs.

4.3 Mean of the absolute value of the error on estimation of the altitude h function of the value of h in meters

Figure 4. Mean of the absolute value of the error on estimation of one of the parameters of interest in WFAO. Uncertainty defined à 3σ where σ is the standard deviation is plotted, computed for a 100 matrix population for each SNR.

The source module is made up with 7x9 unresolved sources in the visible wavelengths (λ =635 $\pm$5 nm) dispatched over a reconfigurable cartesian grid. This leads to a field of view of $427\lambda/D * 484\lambda/D$. The source module is associated with a collimator to simulate Natural Guide Stars. Then light comes through three Kolmogorov type turbulent layers on a rotating stage. A wide field WaveFront Sensor analyses GS.s light. It has 7x7 sub-apertures, each one has 142x142 pixels. A wide field imaging camera is used for performance computation. Correction is performed with two deformable mirrors. Both are magnetic membrane mirrors: a continuous membrane is deformed by the magnets placed in front of solenoids.

The first deformable mirror DM1 is conjugated with the pupil of the system: this DM1 has 52 effective actuators, with a coupling factor of 40%. The second deformable mirror DM2 is placed in a diverging beam, it can be conjugated either to the pupil plane or to altitude thanks to a translation rail (0 km to 16500 km in a VLT-equivalent case). It has 88 effective actuators with a coupling factor of 65%.

3.2 GeMS

GeMS is the Gemini Multi-conjugated adaptive optics System. It is a facility instrument that delivers a uniform, diffraction-limited corrected near-infrared image over a field of view of 2armcin. A detailed description of each sub-system can be found in previous papers.[5,20] In short, a 50W laser is split in 5x10W beacons to produce the 5 laser guide stars (LGS) placed on the sky at the corner and center of a 60 arcsec square. These five LGS are seen by five, 16x16 subapertures, Shack-Hartmann wavefront sensors. The 2040 slope measurements are used to compute the MCAO high-order correction, correction provided at 800Hz by three deformable mirrors conjugated to 0, 4.5 and 9km and totaling 917 actuators. Besides that, up to three either visible or NIR natural guide stars (NGS) provide the measurements for the compensation of the tip-tilt and anisoplanatic modes.

3.3 SAXO

SPHERE (Spectro-Polarimetry High-contrast Exoplanet Research)[21] is an European instrument which will equip one of the four 8-m telescopes of the European Southern Observatory Very Large Telescope at Paranal (Chile). Its main scientific objective is direct detection of exoplanets and their spectral characterization. Such a challenging goal requires a relatively complex high-contrast instrument whose the core is the extreme AO system: SAXO (SPHERE Adaptive optics for eXoplanet Observation). Requierements and a detailed description of the system can be found in previous articles.[1,22,23] We just highlight here the main features, gathered together in table 2.

Wavefront analysis is performed thanks to a 40x40 visible Spatially filtered Shack-Hartmann (VIS-WFS)[24,25] with EMCCD 240x240 pixels working at 1200 Hz and a read out noise smaller than 1 e-. Correction is provided through a high spatial frequencies (41x41 actuators) and high bandwidth deformable mirror manufactured by

Table 1. LGS-WFS and DMs characteristics of GeMS.

WFS location in FoV	Pointing at LGS located at [0",0"]; [-30",+30"] [+30",+30"]; [+30",-30"]; [-30",-30"]
Number of valid subapertures	204 per WFS (total 1020)
Sampling frequency	up to 800Hz
WFS pixel size	1.38"
WFS RON (measured)	3.5e-
LGS Spot Size	1"
4.5km, 9km]	
Number of Actuators	[293 (240 valid), 416 (324 valid), 208 (120 valid)]
Inter-actuator Coupling	[33%, 33%, 33%]
Physical actuator pitch	[5mm, 5mm, 10mm]

Table 2. WFS and DM characteristics of SAXO.

Number of valid subapertures	1240
Sampling frequency	1200 Hz
WFS pixel size	0.36"
WFS RON (measured)	$<$ 1e-
Number of Actuators	1377 (1304 dynamically controlled)
Inter-actuator Coupling	28%
Physical actuator pitch	4.5 mm

CILAS, totaling 1377 actuators with a coupling factor of 28%. A fast (bandwidth at -3db larger than 800 Hz) image Tip-Tilt mirror is used for image motion correction.

Relative alignment specifications between the DM and the WFS are 1/10 sub-aperture in translation and 1/10 edge sub-aperture in rotation.

4. APPLICATION OF THE METHOD

4.1 HOMER: Identification of DM/WFS mis-registration

Considering the HOMER test-bench, we can introduce a known mismatch between the WFS and the DM by translating and/or rotating the micro-lens matrix of the WFS, (but not the camera itself), in order to test the method performance. The translation / rotation introduced are precisely calibrated thanks to the WFS slopes registered at high SNR. For each position WFS slopes are recorded and translation and rotation is computed by the difference between the two sets of slopes. In these low noise conditions slopes variance is 5.10^{-4} pixel^2. Defining the error slopes computation by $3\sigma_{slopes}$ where σ_{slopes} is the slopes standard deviation, the precision on micro-lens matrix displacement estimation is $\sqrt{2} * 3\sigma_{slopes}$, equal to 0.1 pixel that is to say a precision better than 1/1000 sub-aperture since each subaperture has 142x142 pixels. For each position, 10 matrices are computed in different SNR conditions. A joint estimation of the relative translation, the relative rotation and the magnification is then performed using the method.

Results are shown in figure 5. They present the performance achieved by the algorithm for the translation and the rotation estimation, for 3 SNR conditions representative of noise conditions on HOMER : a high SNR (200), a medium SNR (40) and a very poor SNR (4). The plotted error bars correspond to $\pm\sigma$ where σ is the standard deviation of the values estimated by our algorithm based on a 10 matrix population. The function $y = x$ is plotted in dashed line, it goes through all the data points. Identification process is thus linear. For translations lower than 0.5 sub-aperture, the precision is better than 1/100 subaperture, and even for poor SNR condition, it is better than 1/20 subaperture, which is beyond requirements. Performance achieved for rotation estimation is similar. The identified magnification is uniform and equal to 0.988 $\pm$0.002. It is worth noting that performance is similar for a mis-registration composed of a X-Y translation plus a rotation, and that all the different modes are well decoupled.

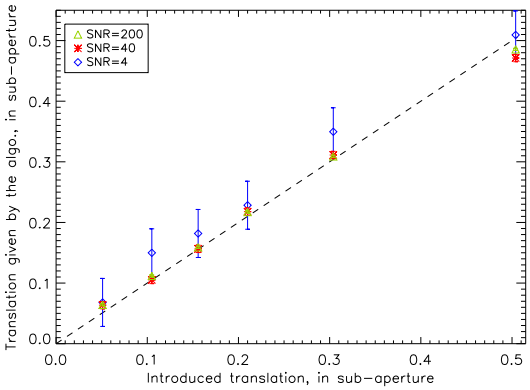

5.1 Relative translation identification

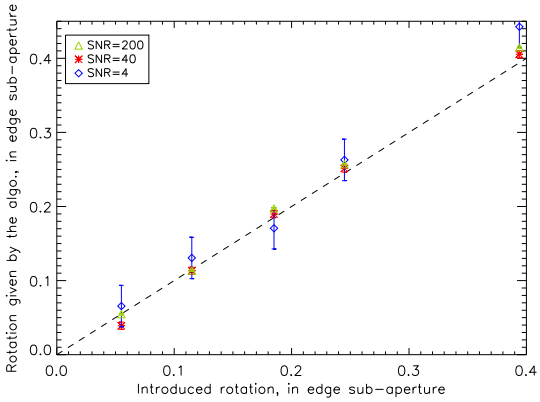

5.2 Relative rotation identification

Figure 5. Experimental results of estimation of the relative translation and rotation between the WFS and the DM in the pupil on Homer bench. Three SNR cases are tested. Error bars represent $\pm$ the standard deviation of the estimated value for a population of 10 iMat.

4.2 SPHERE

The same algorithm has been implemented and validated on the AO bench of SPHERE: Saxo. The procedure is the same as the one applied on the HOMER bench: a known translation is introduced thanks to the WFS that is latter retreived by our method. The precision of the translation induced on the WFS is the one achieved by the translation plate: ± 2 microns (± 0.015 subaperture) because translation is applied to the whole WFS (micro-lens matrix and camera) and not just to the micro-lens matrix as on HOMER. Five iMat based on the classical Hadamard technique are computed at each position, for good SNR conditions.

Identification process uses a binary weight map defined by a threshold of 25% of the maximum value of slopes for each actuator. The identified translation versus the introduced translation is plotted on figure 6.1. The standard deviation calculated on the 5 iMat $= 0.002$ subaperture (better than the precision on the introduced translation). The function $y = x + b$ is plotted in red dashed line, it shows the good linearity of the process, and finding the parameter b leads the identification of the optimal position, here identified to a translation of -0.04 sub-aperture with respect to the actual position.

In order to verify this result, performance in closed-loop is also computed for each relative translation value so we can compare the zero-position given by the algorithm with the position where the performance is the highest. On figure 6.2 the relative loss of performance compared to the initial performance is plotted with respect to the relative translation. A second order fit is computed (red dashed line), whose minimum is found for a relative translation of -0.02 sub-aperture. Taking into account the error bars, it confirms the optimal position computed by the algorithm.

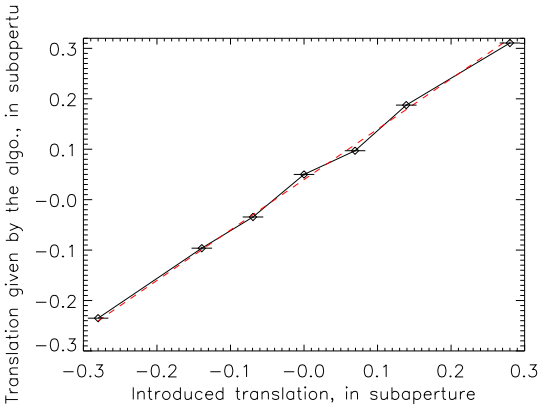

6.1 Relative translation identification on Sphere. The red dashed line is a linear fit.

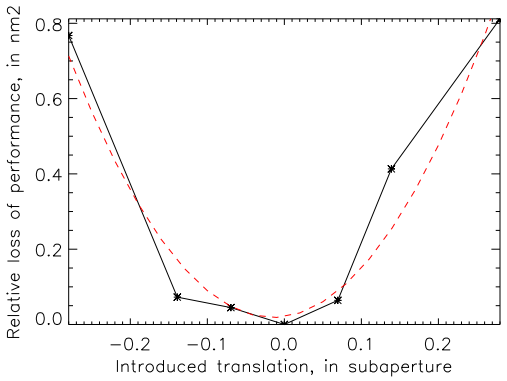

6.2 Loss of performance against the one computed at the reference position, versus the introduced translation. The red dashed line is a 2nd order polynomial fit.

Figure 6. Experimental identification of the relative translation between the DM and the WFS on Sphere

The developed method leads to a precise identification of the mismatch WFS/MD pupil which meets the needs on SAXO: relative translation is identified with a 1/50 sub-aperture precision compared to a requierement of 1/10 sub-aperture.

4.3 GeMS: influence functions, mis-registration and DM altitudes

The same method has been applied for GeMS. In that case we are not introducing fake mis-alignments, but we want to characterize them. In GeMS, the registration between the 5LGSWFS and DM0 is adjusted by the LGSWFS zoom mechanisms. We use a set of two zoom lenses and 5 pupil adjustment mechanisms to minimize the registration on each WFS. The procedure is the following:

1. Close the loop on 1 WFS with DM0 only
2. Remove static focus on DM0 by fine tuning zoom positions
3. Save reference slopes
4. Poke on 9 actuators on DM0 and save slopes
5. compute translation, magnification and rotation
6. adjust pupil mechanism to null translation and magnification
7. Do it iteratively on all the WFS, and while the total magnification is greater than a threshold (usually set to 0.5%)

This procedure allows to center almost perfectly the 5WFS on DM0, however results are not exactly zero as the zoom mechanisms provide 8 degree of freedom, for the 10 (5WFSx2 axis) adjustments to be done. This procedure is ran before grabbing any iMat. iMats are saved based on the classical Hadamard technique, and we also save iMats for different LGS ranges, from 90km to 160km. We then apply the full optimization method on these iMat, trying to identify all the free parameters: IF shape, mis-registration, direction of analysis and DM altitudes. Different analytical forms has been tried for the IF, and we have found that a shape like:

$$IF = sinc(x/a) * sinc(y/a) * exp(-(x/b)^2. - (y/b)^2.)) \tag{8}$$

where a and b are left free during the optimization procedure, gives the best results.

Fig7 shows an example of the fitting process for the central WFS on DM0 and on DM9. The IF fit gives average values of a = 26.2 and b = 8.4, with an rms of respectively 0.5 and 0.2.

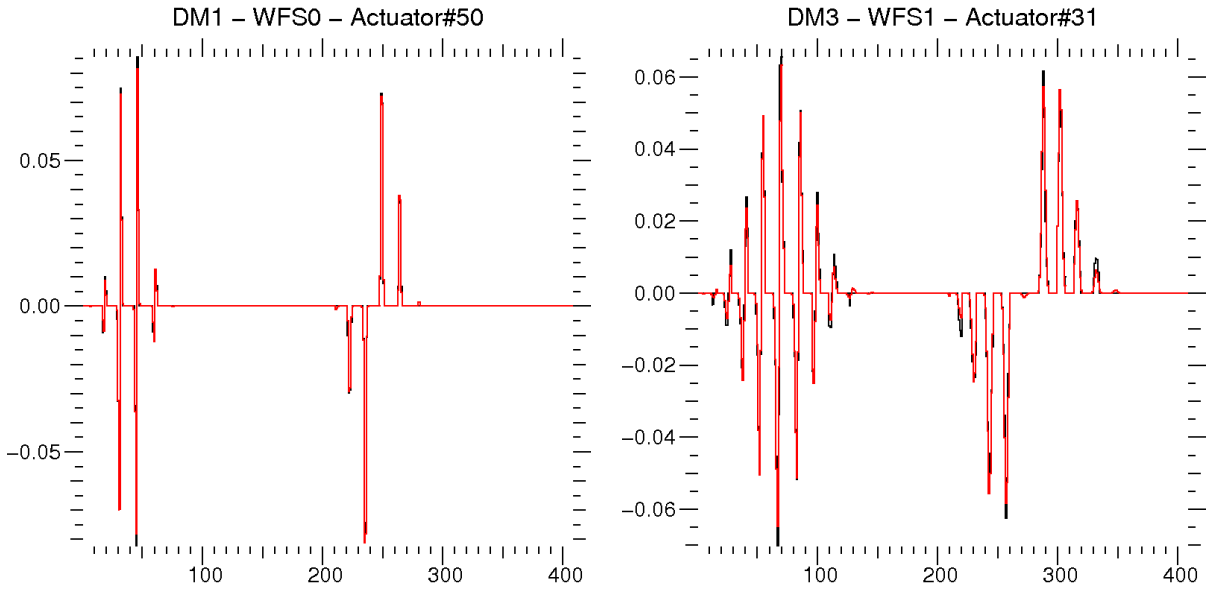

Figure 7. Example of fitting process for an actuator on DM0 (left) and on DM9 (right) seen by the central WFS of GeMS. Black is the experimental iMat and red is the fit result

In Fig. 8 we show the registration map for a WFS with respect to DM0, and the same map once the contribution of the DM has been removed, i.e., when we remove the common Translation/rotation to all WFS. Note that all the bad actuators (i.e. stuck actuators) are removed before doing the projection onto the modes. On Fig.8-right, the residual mis-registration has an rms of 0.3% of an subaperture and a peak value of 1.3%. This is the limitation imposed by the lenslet optical quality, and can not be compensated for.

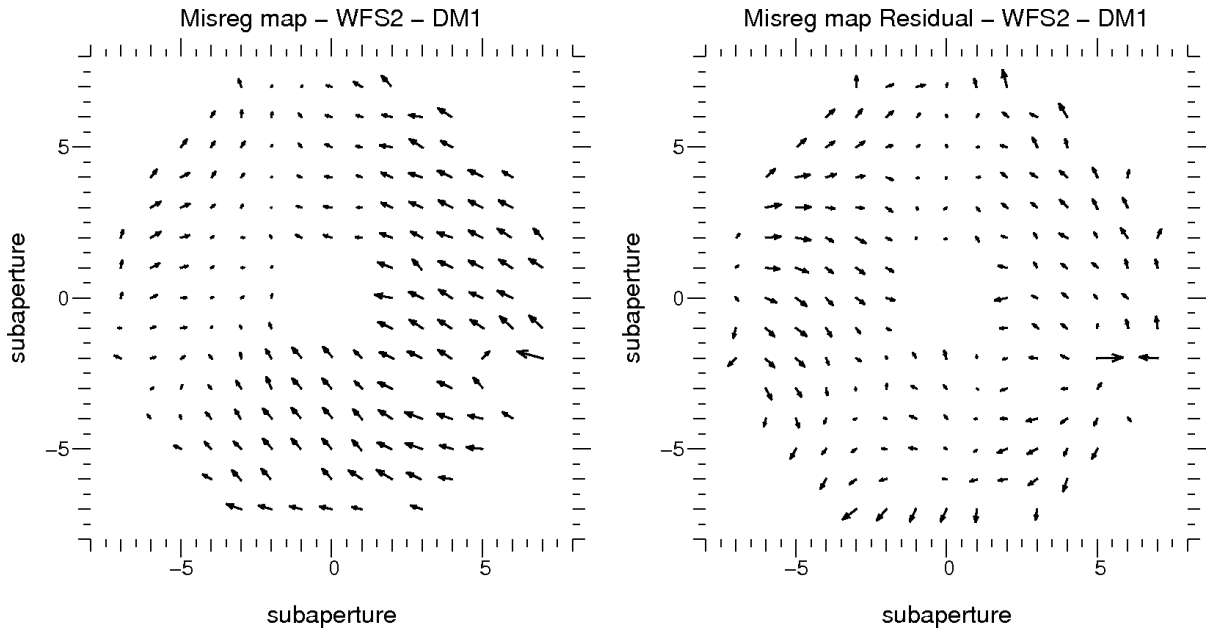

Figure 8. Registration maps as a result of the fitting procedure for a given WFS and DM0. Left: Raw registration. Right: residual registration once the DM part has been subtracted.

For the registration of the 5 WFS with respect to DM0, we find that the global translation is of the order of 2% of a subaperture, which is the result of the limitation of the registration procedure described at the beginning of this section. The average magnification has been optimized by the same procedure, and we check that its value is below the asked threshold of 0.5% (100% magnification is such as the spot falls in the next sub-pupil). Finally, the rotation (and differential rotation) are very small, of the order of 0.03degree. For DM0, the method has been been cross-checked with an independent method based on a waffle pattern used by J.-P. Veran for Altair.[26] Using the same iMat, but this waffle method, results are very similar. Fig.9 shows the correspondence between both methods for the 20 parameters (20 = 4 modes x 5 WFS). No obvious bias are seen.

For the DMs in altitude, we have tried to estimate the altitude and direction errors from the individual mis-registration maps. As GeMS is working with LGS, the altitude error can be identified by a global magnification error. For instance, for the DM conjugated at 9km, and error of +200m in its altitude (if the DM is at 9.2km instead of 9km) would produce a magnification of -0.2% of the total pupil (pupil stretched by 0.2%), which would be 3% of a subaperture. The associated registration error would be 0.03m in X and Y, which is around 6% of a subaperture.
Results for DM0 and DM9 shows almost no individual magnification error: -0.3% for the DM at 4.5 km and -0.5% for the DM at 9km. The global magnification error (i.e. the one derived from the global mis-registration of each WFS) is also indicating a very small error in altitude: 20m for the DM at 4.5km and 40m for the DM at 9km. This is consistent with the WFS individual magnification. For illustration purpose, we can fix the altitude in the fitting process, and use a theoretical iMat that would have been computed with a wrong altitude. For instance, if we use a an altitude of 8.5km for the DM that is conjugated at 9km, we retrieve an offset of 0.06m in X and Y for each WFS which would be equivalent to an error in altitude of ∼450m. We also measure an individual magnification of ∼1%, which is consistent with the artificial altitude shift induced. Still for illustration purpose, we can use a theoretical iMat that would have been computed for a different LGS range. For instance we use a range of 104.3km (equivalent to a telescope elevation of 60degree). This produces a magnification on each WFS of about 1.4%, but no changes in their individual registration is measured.

As stated in sect.2, once we have removed all the DM part, the residual shift per WFS are due to pointing errors. For GeMS the remaining pointing errors for DM4.5 and DM9 are illustrated in Fig. 10.

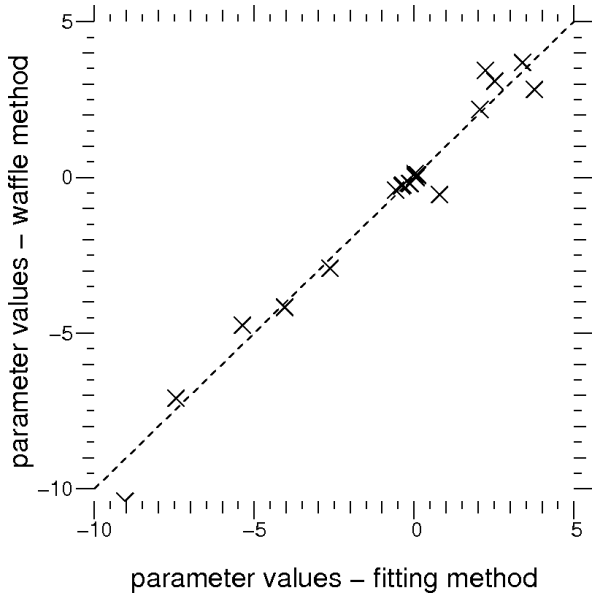

Figure 9. Registration maps as a result of the fitting procedure for a given WFS and DM0. Left: Raw registration. Right: residual registration once the DM part has been subtracted.

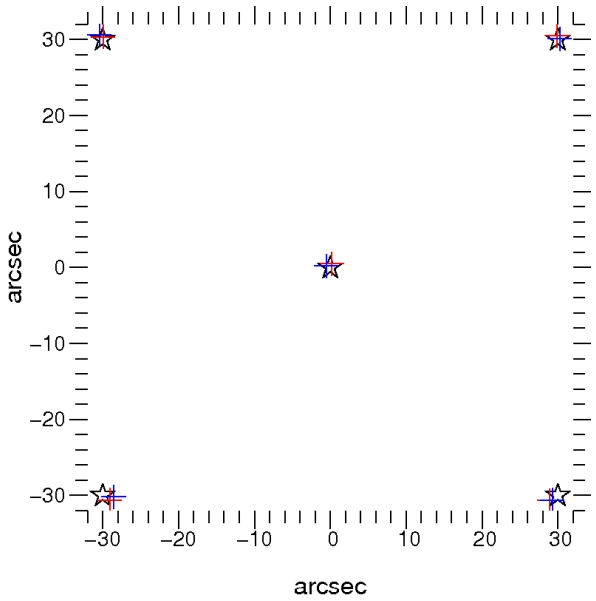

Figure 10. Pointing errors for the 5LGSWFS of GeMS. Stars are the canonical +/- 30arcsec that defines the constellation. Red is the pointing determined from the registration on DM4.5 and blue is from DM9.

Results are consistent for both DMs, even though they are not exactly the same. We believe that this is due the fact that the DM9 has only a small number of actuators which reduce the sensitivity of the method.

In conclusion, we have been able to identify the IF, the lenslet quality, the altitude of the DMs and the WFS pointing directions. All these parameters are used to build the synthetic interaction matrix.

5. CONCLUSION

We have presented a method used for the identification and calibration of the interaction matrix parameters for AO and MCAO systems. The method allows to precisely determine parameters like the influence functions, lenslet optical quality, mis-registration and in the case of MCAO systems: DM altitude and WFS pointing directions. The method has been validated in simulations and on three different AO bench, namely: HOMER, GeMS and SPHERE.

ACKNOWLEDGMENTS

Authors want to acknowledge Jean-Pierre Véran for his participation in this project.The Gemini Observatory is operated by the Association of Universities for Research in Astronomy, Inc., under a cooperative agreement with the NSF on behalf of the Gemini partnership: the National Science Foundation (United States), the Science and Technology Facilities Council (United Kingdom), the National Research Council (Canada), CONICYT (Chile), the Australian Research Council (Australia), Ministério da Ciência e Tecnologia (Brazil) and Ministerio de Ciencia, Tecnología e Innovación Productiva (Argentina).

REFERENCES

[1] Petit, C., Fusco, T., Sauvage, J.-F., Sevin, A., and et al., "Integration, tests and laboratory performance of saxo, the vlt-sphere extreme ao system," in [*2st AO4ELT conference - Adaptative Optics for Extremely Large Telescopes*], Véran, J., Clénet, Y., and Fusco, T., eds., *EDP Sciences* **2** (2012).

[2] S., T., Macintosh, B., Palmer, D., Saddlemyer, L., and et al., "Gemini planet imager: From integration and test to planning observations," in [*American Astronomical Society (AAS) meeting*], AAS, ed., *219* **245**, 14 (2012).

[3] Kasper, M., Fedrigo, E., Looze, D., and Bonnet, H., "Fast calibration of high-order adaptive optics systems," *JOSA-A* **21**, 1004–1008 (2004).

[4] Meimon, S., Fusco, T., and Petit, C., "The slope-oriented hadamard scheme for in-lab or on-sky interaction matrix calibration," in [*2st AO4ELT conference - Adaptative Optics for Extremely Large Telescopes*], Véran, J., Clénet, Y., and Fusco, T., eds., *EDP Sciences* **2** (2012).

[5] Rigaut, F., Neichel, B., and et al., "Gemini south mcao on-sky results," in [*2st AO4ELT conference - Adaptative Optics for Extremely Large Telescopes*], Véran, J., Clénet, Y., and Fusco, T., eds., *EDP Sciences* **2** (2012).

[6] Fusco, T., Meimon, S., Thatte, N., Schnetler, H., and et al., "Laser tomographic ao system for an integral field spectrograph on the e-elt: the atlas project," in [*2st AO4ELT conference - Adaptative Optics for Extremely Large Telescopes*], Véran, J., Clénet, Y., and Fusco, T., eds., *EDP Sciences* **2** (2012).

[7] Fusco, T., Conan, J.-M., Rousset, G., Mugnier, L., and et al., "Optimal wave-front reconstruction strategies for multiconjugate adaptive optics," *JOSA-A* **18**, 2527–2538 (2001).

[8] Kolb, J., [*Calibration and test tools for MCAO systems: Application to the ESO Demonstrator MAD*], Paris VI (2005).

[9] Oberti, S., Quiros-Pacheco, F., Esposito, S., and Muradore, R., "Large dm ao systems: synthetic im or calibration on sky?," in [*Advances in Adaptive Optics II*], Ellerbroek, B. L. and Bonaccini, D., eds., *Proc. SPIE* **6272**, 627220 (2006).

[10] Neichel, B., Fusco, T., and Conan, J.-M., "Tomographic reconstruction for wide-field adaptive optics systems: Fourier domain analysis and fundamental limitations," *JOSA-A* **26**, 219 (2008).

[11] Costille, A. and Fusco, T., "Impact of the cn2 description on wide field ao performance," in [*2st AO4ELT conference - Adaptative Optics for Extremely Large Telescopes*], Véran, J., Clénet, Y., and Fusco, T., eds., *EDP Sciences* **2** (2012).

[12] Cortes, A., Neichel, B., Guesalaga, A., and et al., "Atmospheric turbulence profiling using multiple laser star wavefront sensors," *MNRAS* **accepted for publication** (2012).

[13] Gilles, L. and Ellerbroek, B., "Real-time turbulence profiling with a pair of laser guide star shack-hartmann wavefront sensors for wide-field adaptive optics systems on large to extremely large telescopes," *JOSA-A* **27**, A76 (2010).

[14] Vidal, F., Gendron, E., Brangier, M., Sevin, A., Rousset, G., and Hubert, Z., "Tomography reconstruction using the learn and apply algorithm," in [*1st AO4ELT conference - Adaptative Optics for Extremely Large Telescopes*], Clénet, Y., Conan, J.-M., Fusco, T., and Rousset, G., eds., *EDP Sciences* **1**, 07001 (2010).

[15] Tordo, S., "Integration and alignment of adaptive optics systems: 10 years of experience at the vlt," in [*Adaptive Optics Systems II*], Ellerbroek, B. L., Wizinowich, P., Hart, M., and Hubin, N., eds., *Proc. SPIE* **7736**, 7736 (2010).

[16] Bechet, C., Thiebaut, E., Tallon, M., Kolb, J., and et al., "Identification of system misregistrations during ao-corrected observations," in [*2st AO4ELT conference - Adaptative Optics for Extremely Large Telescopes*], Véran, J., Clénet, Y., and Fusco, T., eds., *EDP Sciences* **2** (2012).

[17] Marquardt, D. W., "An algorithm for least-squares estimation of nonlinear parameters," *Journal of Optical Society for Industrial and Applied Mathematics* **11**, 431–441 (1963).

[18] Parisot, A., Costille, A., Petit, C., and Fusco, T., "Closed-loop tomographic control on homer wide-field ao bench: experimental results and identification issues," in [*Adaptive Optics Systems II*], Ellerbroek, B. L., Wizinowich, P., Hart, M., and Hubin, N., eds., *Proc. SPIE* **7736**, 773637–13 (2010).

[19] Costille, A., Petit, C., Conan, J.-M., Kulcsár, C., Raynaud, H.-F., and Fusco, T., "Wide field adaptative optics laboratory demonstration with closed loop tomographic control," *JOSA-A* **27**, 469–483 (2010).

[20] Neichel, B., Rigaut, F., and et al., "The gemini mcao system gems: nearing the end of a lab-story," in [*Adaptive Optics Systems II*], Ellerbroek, B. L., Wizinowich, P., Hart, M., and Hubin, N., eds., *Proc. SPIE* **7736**, 7736 (2010).

[21] Beuzit, J.-L., Mouillet, D., Moutou, C., Dohlen, K., Puget, P., Fusco, T., and Boccaletti, A., "A planet finder instrument for the vlt," *Proceedings of IAU Colloquium 200, Direct Imaging of Exoplanets: Science & Techniques, Cambridge University Press* , 317–323 (2005).

[22] Fusco, T., Rousset, G., Sauvage, J.-F., Petit, C., Beuzit, J.-L., Dohlen, K., and et al., "High order adaptive optics requirements for direct detection of extra-solar planets. application to the sphere instrument," *Opt. Express* **14**(17), 7515–7534 (2006).

[23] Petit, C., Fusco, T., Charton, J., Mouillet, D., Rabou, P., Buey, T., Rousset, G., Baudoz, P., P.Gigan, Kasper, M., Fedrigo, E., Hubin, N., Feautrier, P., Beuzit, J.-L., and Puget, P., "The sphere xao system: Design and performance," in [*Adaptive Optics Systems*], Hubin, N., Max, C., and Wizinowich, P., eds., *Proc. SPIE* **7015**, 70151U (2008).

[24] Poyneer, L. A. and Macintosh, B., "Spatially filtered wave-front sensor for high-order adaptive optics," *JOSA-A* **21**, 810.819 (2004).

[25] Fusco, T., Petit, C., Rousset, G., Conan, J.-M., and Beuzit, J.-L., "Closed-loop experimental validation of the spatially filtered shack-hartmann concept," *Opt. Letters* **30**(11), 1255–1257 (2005).

[26] Oliker, M., "Alignment techniques for dm, lenslet, and wfs camera at the sor," in [*Adaptive Optics and Applications*], Tyson, R. K. and Fugate, R. Q., eds., *Proc. SPIE* **3126**, 3126 (1997).